PROCEEDINGS OF SPIE

SPIEDigitalLibrary.org/conference-proceedings-of-spie

Tunable and reconfigurable high-index semiconductor meta-optics

Lewi, Tomer, Butakov, Nikita, Iyer, Prasad, Evans, Hayden, Chorsi, Hamid, et al.

Tomer Lewi, Nikita A. Butakov, Prasad P. Iyer, Hayden A. Evans, Hamid Chorsi, Juan Trastoy, Javier Del Valle Granda, Ilya Valmianski, Christian Urban, Yoav Kalcheim, Ivan K. Schuller, Jon A. Schuller, "Tunable and reconfigurable high-index semiconductor meta-optics," Proc. SPIE 11290, High Contrast Metastructures IX, 112901B (26 February 2020); doi: 10.1117/12.2545075

Event: SPIE OPTO, 2020, San Francisco, California, United States

Tunable and Reconfigurable High-index Semiconductor Meta-optics

Tomer Lewi[a*], Nikita A. Butakov[b], Prasad P. Iyer[b], Hayden A. Evans[d], Hamid Chorsi[b], Juan Trastoy[c,e], Javier Del Valle Granda[c], Ilya Valmianski[c], Christian Urban[c], Yoav Kalcheim[c], Ivan K. Schuller[c] and Jon A. Schuller[b]

[a]*Faculty of Engineering and Institute for Nanotechnology and Advanced Materials, Bar-Ilan University, Ramat-Gan 5290002, Israel*
[b]*Department of Electrical & Computer Engineering, University of California Santa Barbara, Santa Barbara, California 93106, United States*
[c]*Department of Physics, University of California, San Diego, La Jolla, California 92093, United States*
[d]*Materials Research Laboratory and Department of Chemistry and Biochemistry, University of California Santa Barbara, California 93106, United States*
[e] *Unité Mixte de Physique CNRS, Thales, Univ. Paris-Sud, Univ. Paris Saclay, 91767 Palaiseau, France*

Abstract

Metasurfaces manipulate light through engineering the amplitude, phase and polarization across arrays of meta-atom antenna resonators. Adding tunability and active functionality to metasurface components would boost their potential and unlock a vast array of new application possibilities such as dynamic beam steering, LIDAR, tunable metalenses, reconfigurable meta-holograms and many more. We present here high-index reconfigurable meta-atoms, resonators and metasurfaces that can dynamically and continuously tune their frequency, amplitude and phase, across the infrared spectral ranges. We utilize narrow linewidth resonances along with peak performance of tunable mechanisms for efficient and practical reconfigurable devices.

Keywords: Dielectric Mie resonators, nanoparticles, tunable metasurfaces, reconfigurable metasurfaces, phase change materials

1. INTRODUCTION

Metasurfaces are two-dimensional structures designed to manipulate light through arbitrary wavefront shaping [1] [2] [3] [4]. Recently a lot of attention in the field has shifted to the realization of all-dielectric metasurfaces and has led to tremendous progress, giving rise to several demonstrations including achromatic and broadband metalenses [5] [6] [7], axicon lenses[8], sub-diffraction focusing[9], nonlinear generation[10] [11] [12] beam deflectors[8,13] [14], wave plates and beam converters [15] [16] [17] [18], holograms[19] [20] [21], antireflection coatings[22] and magnetic mirrors[23], to name a few. However, most metasurfaces are still implemented for static operation and optimized for limited bandwidth of operation. The next frontier lies in dynamic and active control over light, which will drastically increase metasurface capabilities and potential applications.

The fundamental challenge for achieving reconfigurable operation is to obtain large and continuous modulation of optical properties within subwavelength meta-atoms and meta-molecules which are inherently low-Q resonators[24,25]. Desirable tuning mechanisms continuously shift the resonance frequency of the metastructure with at least one linewidth of the resonance, thus allowing to maximize the modulation of both amplitude and phase. These challenges have motivated several studies exploring different approaches, designs, and materials that provide extreme tunability. Previous investigations of active tuning in dielectric metasurfaces and meta-atoms have focused on ultrafast free-carrier injection[26,27], coupling to liquid crystals[28,29], to atomic vapor[30] or to ENZ materials[31,32], phase change materials[33,34] and MEMS[35] [36] [37] . However, most of these approaches do not provide a viable solution for a fully reconfigurable metadevice where at each subwavelength meta-atom the phase and amplitude can be individually and continuously tuned to provide an arbitrary phase profile. Recent studies have showed that the thermo-optic effect (TOE), i.e. refractive index variation with temperature dn/dT can be used to induce large and continuous index shifts in materials having extraordinary

[*] *E-mail: tomer.lewi@biu.ac.il

High Contrast Metastructures IX, edited by Connie J. Chang-Hasnain, Andrei Faraon, Weimin Zhou, Proc. of SPIE Vol. 11290, 112901B · © 2020 SPIE · CCC code: 0277-786X/20/$21 · doi: 10.1117/12.2545075

thermal dependence[38 39 40,41]. The TOE was also recently used to actively tune Si metasurfaces, but only at a limited temperature range (273-573K)[42]. Here we present free carrier and thermal tunability in several groups of high-index semiconductor resonators over large MIR spectral ranges. We demonstrate doping dependent tuning of Mie resonances in Si due to modulation of carrier densities. Next we study thermal and TO tunability in group IV semiconductors (Si and Ge) due to the normal positive TOE (dn/dT >0) and in the lead chalcogenide family of group IV-VI semiconductors (PbTe) due to the anomalous dn/dT <0 . We demonstrate the tuning of high order mid-infrared (MIR) Mie resonances by several linewidths with temperature swings as small as ΔT<10K. Lastly, we discuss reconfigurable and switchable devices driven by metal-insulator transitions in vanadium-oxide (VO_2). We demonstrate independent and continuous tuning of both amplitude and phase in a single electrically controlled nanophotonic device based on Ge on VO_2.

Thermo-optic (TO) effects provide an ideal test bed for demonstrating and elucidating reconfigurable metasurface properties. TO tuning can provide large index shifts with no added losses and be integrated into electrically-controlled architectures. Thus, TO tunability forms the basis for many reconfigurable integrated photonic devices. However, the TOC of most materials is small for subwavelength applications, hence typical TO applications exploit small index changes acting over distances much larger than a wavelength to achieve useful modulation. For efficient modulation of subwavelength resonators, the maximally induced index shift Δn should tune the resonance wavelength by more than its linewidth (Δλ/FWHM>1, where Δλ is the resonance wavelength shift and FWHM is the full width at half max of the linewidth). The route for achieving this tunability is by maximizing the TOE using extraordinary materials[24,38,39-41,43,44] and/or narrowing the resonance linewidth using high-Q modes[38] such as supported by asymmetric[28] or fano-resonant[10] metasurfaces.

2. RESULTS AND DISCUSSION

This study of resonator and metasurface tunability is mainly focused for the MIR spectral range which has tremendous scientific and technological interest including nanospectroscopy[45], thermal imaging[46], chemical and biological sensing[47-50], medical applications[51], laser countermeasures[52] and spectro-interferometry for astro-photonics[53-60], to name a few. Importantly, thermal tunability can be extended to the NIR and visible ranges where the performance of e.g. Si and Ge, can be improved due to the expected increase of dn/dT at shorter wavelengths.

Group IV semiconductors

Here we first study the free carrier effects of Si spherical resonators. Varying the carrier concentration in the resonators through doping, we demonstrate blue shifting of Mie resonances for increasing the carrier deinsity[24]. Figure 1 presents the spectral characteristics of Si spheres with a constant radius of d=1 μm with increasing doping concentrations, from undoped Si (blue) and up to highly doped Si of $n=1 \times 10^{20}$ cm^{-3}, demonstrating blue-shifts and broadening of the Mie resonances with increased carrier density. For doping of 3.8×10^{19} cm^{-3} the material behaves like a low index dielectric with overlapping ED and MD modes. For the highest doped sample (pink), the permittivity is negative at long wavelengths, leading to the emergence of an ED plasmonic mode. Nevertheless, resonances are shifted by more than a linewidth with carrier densities > 1×10^{19}.

Next we move to study thermal effects leading to large normalized tunability (more than a linewidth). We start with TO tuning capabilities of Ge – one of the most commonly used materials for dielectric metasurfaces and nanophotonics. The TOC of Ge is amongst the highest of natural materials[61] which, along with its high refractive indices and CMOS compatibility, makes it very attractive materials for reconfigurable metasurfaces. However, the typical TOC value (~5×10^{-4} K^{-1}) requires large temperature modulation which may cause problems if the TOC is strongly temperature dependent[38 39]. In the mid-infrared (MIR) range, for instance, working at high temperatures can generate FC densities in semiconductors that dramatically alter the optical constants due to Drude-like dispersion[62].

To investigate thermal tunability and assess its capabilities, we start by studying Ge single spherical meta-atom resonators fabricated by laser ablation[24,63]. Figure 2 presents a typical spectral response of a Ge spherical Mie resonator with r= 1.75 μm. Experimental spectra (black) show good agreement with the calculated Mie scattering (red) cross-sections σ_{sca} normalized to the geometric cross-section σ_{geo}. A series of multipolar resonance peaks are visible in the spectra and correspond to magnetic dipole (MD), electric dipole (ED) and magnetic (MQ) and electric quadrupole (EQ), respectively. In Figure 3 we focus on the TO tunability of the EQ mode since its Q-factor is relatively high Q_f~50. Temperature dependent spectra of the EQ resonance are illustrated in Figure 3a. Significant red shifts of resonances are observed which provide tuning by more than one resonance linewidth across the 80-573K temperature range.

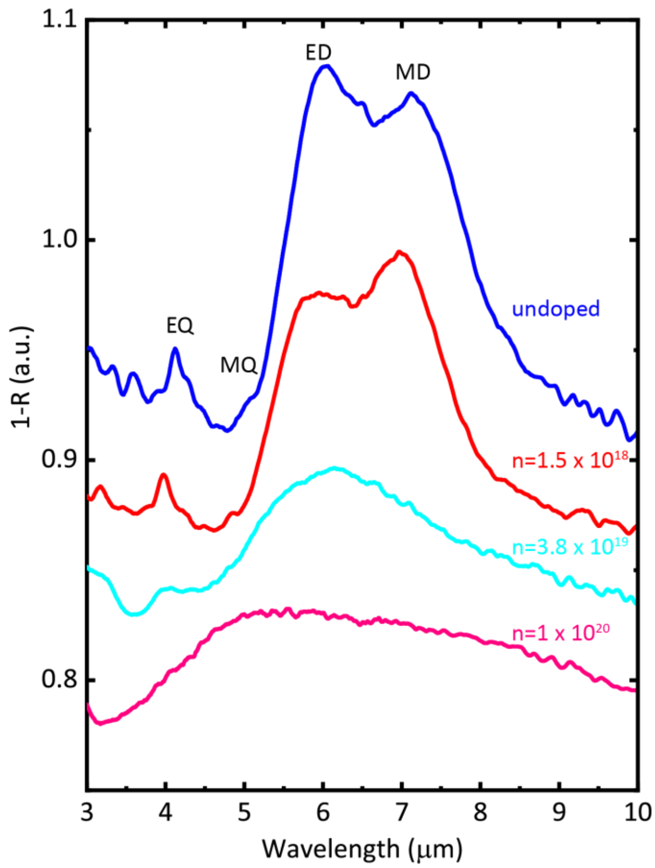

Figure 1: Spectral characteristics of doped Mie resonators and free carrier based tuning effects. The Spectra of 2 μm diameter Si spheres with different doping concentrations, demonstrating blue-shifts and broadening of the Mie resonances with increased doping. For doping of 3.8×10^{19} cm^{-3} the material behaves like a low index dielectric with overlapping ED and MD modes. For the highest doped sample (pink), the permittivity is negative at long wavelengths, leading to the emergence of an ED plasmonic mode.

Figure 3b presents a zoom in view on the spectral shifts between 293K and 473K depicting a normalized tunabiltiy of $\Delta\lambda$/FWHM=1.2 with a temperature gradient of ΔT=180K. Such tunability with a practical temperature difference of ΔT=180K, would be useful for implementing reconfigurable high-Q Ge metasurfaces.

Group IV-VI semiconductors

Although TOCs of group-IV such as Si and Ge are amongst the highest of natural materials[61], achieving the desired tunability ($\Delta\lambda$/FWHM>1) in Si and Ge metasurface requires large temperature gradients. Meeting the desired linewidth tunability with relaxed temperature modulation, requires materials with higher TOCs and/or narrowing the resonance linewidth. Remarkably, the lead chalcogenide family PbX (X=S, Se, Te) possesses both very large refractive indices with highest reported values of TOCs[64].

Figure 4 presents the TO tuning of a high order high-Q (Q~100) Mie resonance in a spherical r=0.9 μm resonator. The high figure of merit of normalized tunability arises due to the high refractive index of the material (n_{PbTe}~6) and large TOC. Interestingly, the sign of the TOC in PbTe is negative (dn/dT<0) due to anomalous temperature-dependent bandgap dispersion[61,65,66]. Combining the large low-temperature TOE with high-Q resonances enables complete tuning (i.e. by more than one linewidth) of resonances with significantly reduced temperature swings (ΔT). This sharp resonance can be tuned by more than one linewidth (normalized tunability=1.02) with a temperature swing as small as ΔT=80K. This large tunability is enabled by the combination of the narrow linewidth and large TOE.

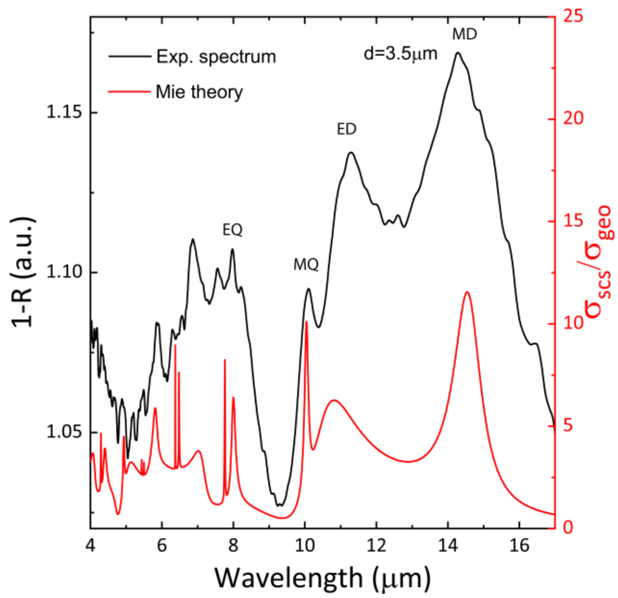

Figure 2: Ge spherical Mie resonator with r= 1.75 µm. Experimental spectra (black) show good agreement with the calculated Mie scattering (cyan, dashed) and FDTD (solid cyan) cross-sections σsca normalized to the geometric cross-section σ_{geo}. A series of multipolar resonance peaks are visible in the spectra and correspond to magnetic dipole (MD), electric dipole (ED) magnetic quadrupole (MQ) and electric quadrupole (EQ), respectively.

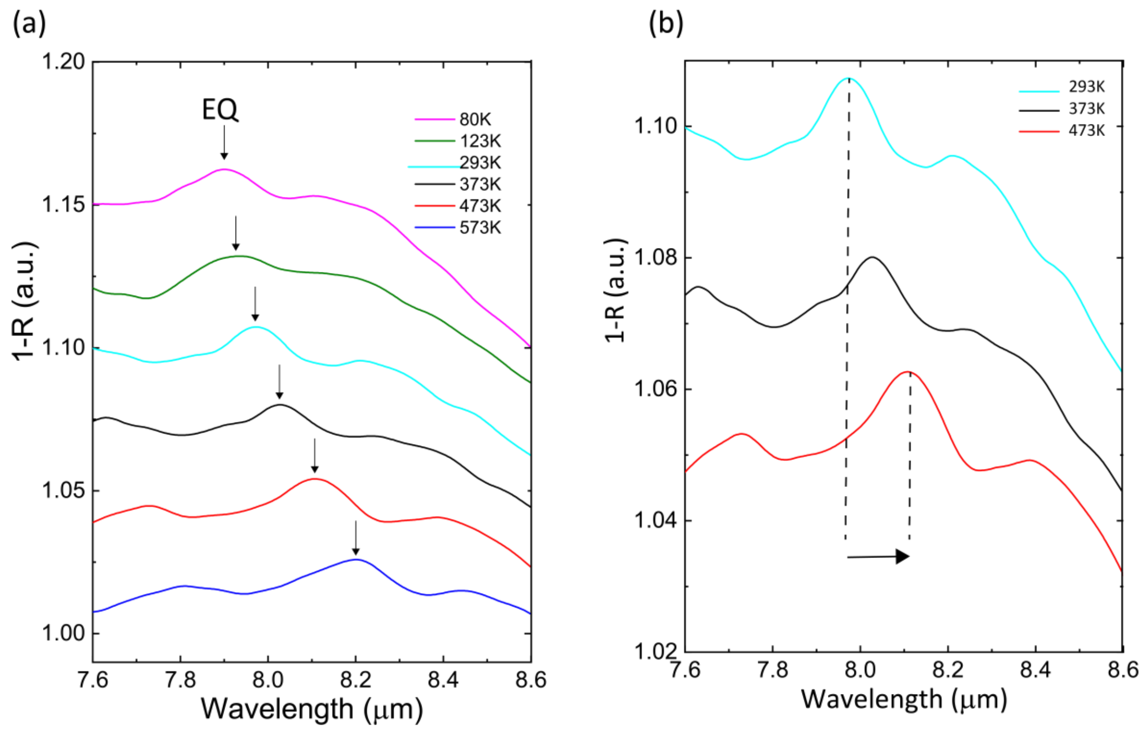

Figure 3: Thermal tuning of a high order EQ in a r=1.75µm Ge spherical resonator (a) Temperature dependent spectra in the 80-573K range (b) Tuning by more than one resonance linewidth (Δλ/FWHM=1.2) with a ΔT=180K temperature gradient demonstrated between 293K and 473K.

Furthermore, at lower temperatures of ~ 170K the observed dn/dT was shown to be an order of magnitude larger than the dn/dT at RT temperatures[38]. These results clearly demonstrate the strong, negative TO effect in PbTe nanoparticles

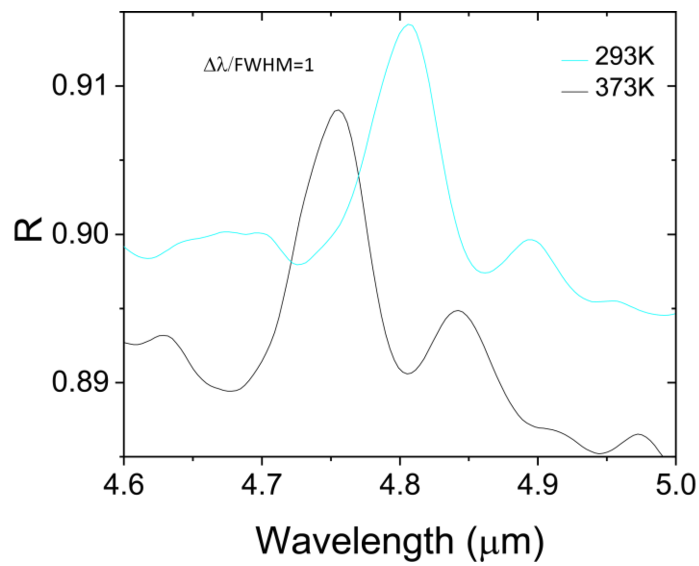

Figure 4: Tunable PbTe meta-atoms. Tuning of high order resonance by more than a linewidth in PbTe spherical resonators with ΔT=80K. At T=173K normalized tunability Δλ/FWHM=1.6 is achieved with ΔT=10K thanks to peak TO coefficient.

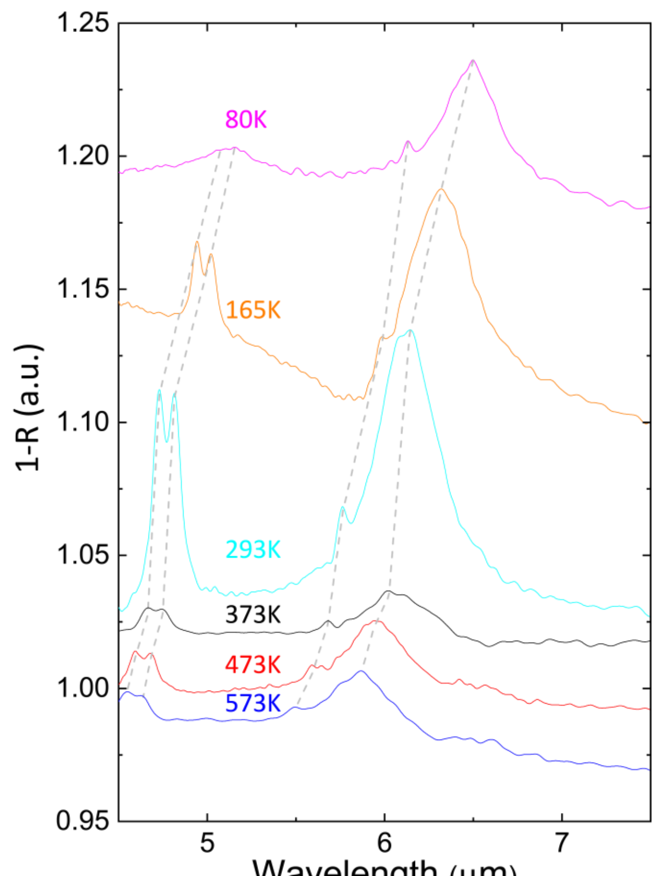

Figure 5: Dynamic tuning in PbTe cubic resonators. Temperature dependent resonance shifts of the first 4 resonance modes in a *a = 850nm* PbTe cube on Au, are presented. The dashed lines are a guide to the eye. Resonance shifts exhibit the large and anomalous (dn/dT < 0) TO coefficient, and a marked increase in magnitude below room temperature.

and is the largest dynamic tuning of Mie resonators reported to date[67-70]. These properties make PbTe an ideal candidate material for TO-tunable nanophotonics and metasurface resonators.

Tracking the shift of all Mie resonances across a variety of temperatures provides valuable insight into the dispersion of TOE with temperature and wavelength. An example of temperature dependent spectra of a PbTe cube of side a=850 nm on a gold substrate, is presented in Figure 5. The temperature dependence of the first 4 resonance wavelengths are tracked. The tunable resonances exhibit some unusual characteristics. The wavelength shifts at low temperatures (80K-293K) are much larger than the shifts above room temperature (293K-573K). These results show that the largest dn/dT occurs between 80K to RT and a more thorough examination reveals a maximum in dn/dT somewhere between 80K and 200K[38]. Although observed shifts are consistent with other measurements[65 71 72], this significant increase in TO coefficient at low temperatures has not previously been reported. Moreover, standard TO models[61], based on temperature-dependent bandgap (E_g) dispersion,[66 73] are unable to explain this effect, suggesting unknown physical mechanisms may be at play. Nevertheless, by operating at cryogenic temperatures, significant increases in TO tunability can be achieved. Altogether these results reveal a great potential for practical TO switching with PbTe components.

Phase transition materials

Among active materials, phase transition and phase change materials can arguably provide the largest variation in optical constants. When applying heat, electric or magnetic fields to these materials, their optical constants can undergo dramatic (and reversible) shifts. Various mechanisms have been investigated and employed to realize tunable nanophotonic and metasurface platforms. These include the transition from nematic to isotropic phases in liquid crystals[28,67], amorphous to crystalline phase change in GeSbTe (GST)[46,74,75] and metal–insulator transitions (MIT) in prototypical strongly correlated materials such as vanadium dioxide (VO_2)[63,76-80] and V_2O_3[81,82].

We have previously demonstrated that VO_2 metasurfaces support switchable dielectric-plasmonic response[63]: in the insulating phase, the metasurfaces exhibit dielectric Mie-type resonances, that are switched to plasmonic resonances in the metallic phase.

In the following, we show that hybrid dielectric–VO_2 structures exhibit several novel behaviors of great interest in the development of reconfigurable optics, including independent tuning of the reflection amplitude and phase, large modulation of transmission and absorption, and electronic switching. Our device is basically a tunable Fabry–Pérot (TFP) cavity, comprised of a 1 µm thick Ge layer, atop of a 100 nm thick film of VO_2, on an R-cut sapphire substrate (Figure 6a). At the interface between a transparent material and VO_2, the reflectivity undergoes a π phase shift across the MIT. Here, reflection-phase switching of the MIT, modulates the complex reflectivity (i.e., amplitude and phase), transmission, and absorption of the simple Ge–VO_2 TFP. Unlike existing switchable VO_2 photonic devices, here the mesoscopic continuous nature of the MIT in the VO_2 thin film, is used to achieve continuous reflection modulation (Figure 6b), as well as independent control over the phase[83], a key requirement for reconfigurable high-efficiency metasurfaces. In Figure 6b and 6c, we demonstrate an electrically controlled TPF device. The device is modulated through Joule heating by passing current directly through a 200 µm × 200 µm TFP. In the VO_2 insulating state, current passes predominantly through the lightly doped Ge layer. This enables Joule heating of the device in both metallic and insulating VO_2 states, without introducing additional lossy metals. The temporal characteristics of the device are investigated by exciting the TFP with a square voltage pulse (26 Vpp, 60 µs), and monitoring the temporal response of the device with a fast MCT detector and the FTIR in a step-scan mode. Transient reflectivity measurements in the 900-3000cm^{-1} range were also carried out, exhibiting the continuous temporal evolution of the spectrum, including the nodes and antinodes. Figure 5c traces the rise and decay time characteristics of at λ=4.7µm. Fast rise time, due to rapid Joule heating is observed, followed by a slower thermal-diffusion-limited decay. Dynamic traces exhibit an approximately 12.6 µs rise time, as determined through an exponential fit with an approximately 285 µs decay time, corresponding to estimated modulation rates on the order of 3.5 kHz. When applying even larger voltages, faster rise times can be achieved[44]. These values are an order of magnitude faster than previous large-area VO_2 optical modulators[79,80] which have rise and relaxation times of the order of few milliseconds. The decay time is likely limited by the relatively large thermal capacitance of the device and may be improved with thermally engineered metasurface structures that reduce the Ge and VO_2 volumes. Further improvements in speed can also be attained by reducing the modulation depth or by utilizing vertical contact geometries.

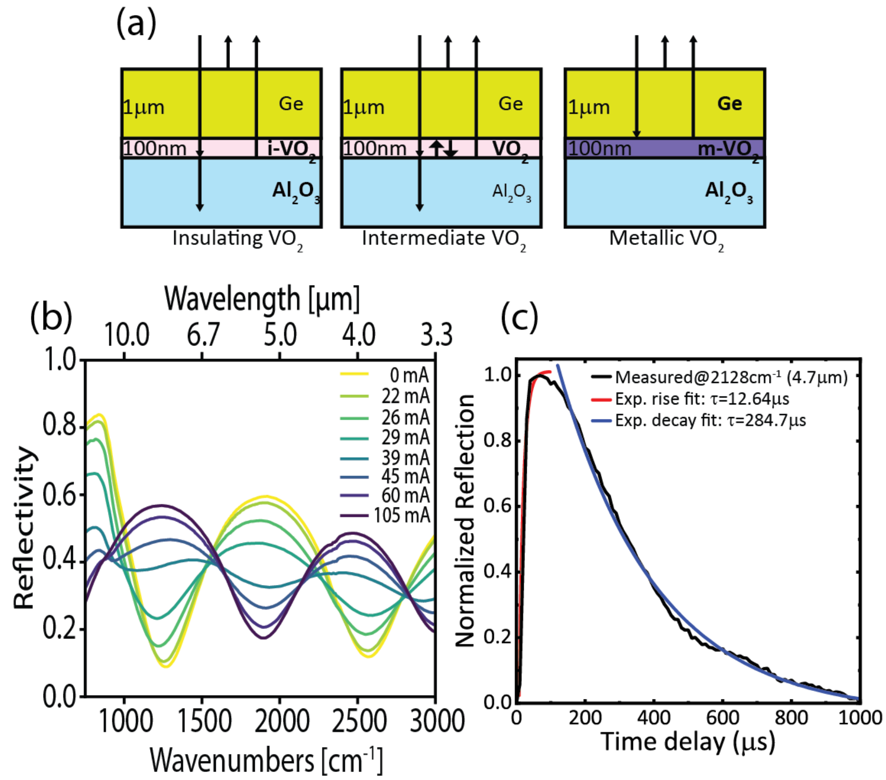

Figure 6: Electrically tunable Fabry–Pérot resonator. (a) Schematic of Ge–VO_2–Al_2O_3 device in the insulating, intermediate, and metallic states. The arrows represent the dominant reflection interfaces. (b) Electrically tuned device, showing continuously modulated reflection amplitude with increase current. (c) Normalized transient reflectivity at the anti-node wavelength (λ = 4.7μm). Solid black line corresponds to the experimental raw data while the red and blue lines correspond to fitted exponential curves (red, heating; blue, cooling).

3. CONCLUSIONS

In summary, we studied dynamic tuning performance in resonators and metasurfaces obtained from several materials systems comprising group IV, group IV-VI semiconductors and phase transition materials. Identifying the linewidth tunability (Δλ/FWHM>1) as the figure of merit for efficient tuning, we pinpoint the route to achieve such tunability by combings materials with large optical effects along with high-Q resonances. We study TO tuning in Ge resonators and highlight their capabilities with a demonstration of tunable high-order resonances which are completely tuned ΔT=180K.

To further reduce the temperature gradients required for linewidth tunability, we investigate lead chalcogenides of group IV-VI semiconductors. We show that PbTe is an excellent candidate for infrared reconfigurable meta-optics, having both high refractive index and largest known TOC of all materials. We find that PbTe exhibits an anomalous TOE with peak performance at cryogenic temperatures, which cannot be explained with standard TOC models.

Finally, we investigate tunability in hybrid dielectric–VO_2 structures and show that these structures exhibit novel properties highly desirable for reconfigurable meta-optics. We utilize the metal–insulator phase transition of VO_2 to create electrically reconfigurable, continuously tunable nanophotonic devices across a broad spectral range. The continuous modulation is enabled by driving the underlying VO_2 film across the phase transition. Electronically triggered transient reflection measurements revealed switching rates of 3.5KHz, which can be further improved with thermal management and more sophisticated designs. These findings expand the potential of active metasurfaces, that take advantage of the reconfigurable properties of hybrid semiconductor–VO_2 architectures. Altogether, this work highlights the opportunities and potential of thermally tunable semiconductor metasurfaces and can pave the way to efficient high-Q reconfigurable metadevices, which will ultimately be implemented in important applications for the infrared range.

Conflicts of interest

There are no conflicts to declare

Acknowledgments:

This work was supported by the Air Force Office of Scientific Research (FA9550-16-1-0393 and FA9550-12-1-0381), by the UC Office of the President Multicampus Research Programs and Initiatives (MR-15-328528), and by a National Science Foundation CAREER award (DMR-1454260). This work was also supported by the Israel Science Foundation (ISF) personal research grant (grant # 205418). Numerical calculations were performed on the computing cluster at the Center for Scientific Computing from the California NanoSystems Institute at the University of California, Santa Barbara: an NSF MRSEC (DMR-1121053) and NSF CNS-0960316. We acknowledge support from the Vannevar Bush Faculty Fellowship program sponsored by the Basic Research Office of the Assistant Secretary of Defense for Research and Engineering and funded by the Office of Naval Research through grant N00014-15-1-2848. Thin films were prepared at the UCSD Nanoscience Center, and nanostructures were fabricated at the UCSB Nanofabrication Facility. This research was conducted with government support under the DoD, Air Force Office of Scientific Research, National Defense Science and Engineering Graduate (NDSEG) Fellowship, 32 CFR 168a. This work was also funded by NG Next, Northrop Grumman Corporation.

References

1 Yu, N. F. *et al.* Light Propagation with Phase Discontinuities: Generalized Laws of Reflection and Refraction. *Science* **334**, 333-337, doi:10.1126/science.1210713 (2011).

2 Jahani, S. & Jacob, Z. All-dielectric metamaterials. *Nature nanotechnology* **11**, 23-36, doi:10.1038/nnano.2015.304 (2016).

3 Kuznetsov, A. I., Miroshnichenko, A. E., Brongersma, M. L., Kivshar, Y. S. & Luk'yanchuk, B. Optically resonant dielectric nanostructures. *Science* **354**, doi:10.1126/science.aag2472 (2016).

4 Arbabi, A., Horie, Y., Bagheri, M. & Faraon, A. Dielectric metasurfaces for complete control of phase and polarization with subwavelength spatial resolution and high transmission. *Nature nanotechnology* **10**, 937-U190, doi:10.1038/Nnano.2015.186 (2015).

5 Aieta, F., Kats, M. A., Genevet, P. & Capasso, F. Applied optics. Multiwavelength achromatic metasurfaces by dispersive phase compensation. *Science* **347**, 1342-1345, doi:10.1126/science.aaa2494 (2015).

6 Khorasaninejad, M. *et al.* Metalenses at visible wavelengths: Diffraction-limited focusing and subwavelength resolution imaging. *Science* **352**, 1190-1194, doi:10.1126/science.aaf6644 (2016).

7 Arbabi, E., Arbabi, A., Kamali, S. M., Horie, Y. & Faraon, A. Controlling the sign of chromatic dispersion in diffractive optics with dielectric metasurfaces. *Optica* **4**, 625-632, doi:10.1364/Optica.4.000625 (2017).

8 Lin, D. M., Fan, P. Y., Hasman, E. & Brongersma, M. L. Dielectric gradient metasurface optical elements. *Science* **345**, 298-302, doi:DOI 10.1126/science.1253213 (2014).

9 Yuan, G. H., Rogers, E. T. F. & Zheludev, N. I. Achromatic super-oscillatory lenses with sub-wavelength focusing. *Light-Sci Appl* **6**, doi:ARTN e17036 10.1038/lsa.2017.36 (2017).

10 Yang, Y. M. *et al.* Nonlinear Fano-Resonant Dielectric Metasurfaces. *Nano letters* **15**, 7388-7393, doi:10.1021/acs.nanolett.5b02802 (2015).

11 Smirnova, D. & Kivshar, Y. S. Multipolar nonlinear nanophotonics. *Optica* **3**, 1241-1255, doi:10.1364/optica.3.001241 (2016).

12 Liu, S. *et al.* Resonantly Enhanced Second-Harmonic Generation Using III-V Semiconductor All-Dielectric Metasurfaces. *Nano letters* **16**, 5426-5432, doi:10.1021/acs.nanolett.6b01816 (2016).

13 Sell, D., Yang, J. J., Doshay, S., Zhang, K. & Fan, J. A. Visible Light Metasurfaces Based on Single-Crystal Silicon. *Acs Photonics* **3**, 1919-1925, doi:10.1021/acsphotonics.6b00436 (2016).

14 Arbabi, A., Arbabi, E., Horie, Y., Kamali, S. M. & Faraon, A. Planar metasurface retroreflector. *Nat Photonics* **11**, 415-+, doi:10.1038/Nphoton.2017.96 (2017).

15 Chong, K. E. *et al.* Polarization-Independent Silicon Metadevices for Efficient Optical Wavefront Control. *Nano letters* **15**, 5369-5374, doi:10.1021/acs.nanolett.5b01752 (2015).

16 Decker, M. *et al.* High-Efficiency Dielectric Huygens' Surfaces. *Adv Opt Mater* **3**, 813-820, doi:10.1002/adom.201400584 (2015).

17 Yang, Y. M. *et al.* Dielectric Meta-Reflectarray for Broadband Linear Polarization Conversion and Optical Vortex Generation. *Nano letters* **14**, 1394-1399, doi:Doi 10.1021/Nl4044482 (2014).

18 Shalaev, M. I. *et al.* High-Efficiency All-Dielectric Metasurfaces for Ultracompact Beam Manipulation in Transmission Mode. *Nano letters* **15**, 6261-6266, doi:10.1021/acs.nanolett.5b02926 (2015).

19 Devlin, R. C., Khorasaninejad, M., Chen, W. T., Oh, J. & Capasso, F. Broadband high-efficiency dielectric metasurfaces for the visible spectrum. *Proceedings of the National Academy of Sciences of the United States of America* **113**, 10473-10478, doi:10.1073/pnas.1611740113 (2016).

20 Li, Z. *et al.* Dielectric Meta-Holograms Enabled with Dual Magnetic Resonances in Visible Light. *ACS nano* **11**, 9382-9389, doi:10.1021/acsnano.7b04868 (2017).

21 Xie, Z. *et al.* Meta-Holograms with Full Parameter Control of Wavefront over a 1000 nm Bandwidth. *Acs Photonics* **4**, 2158-2164, doi:10.1021/acsphotonics.7b00710 (2017).

22 Spinelli, P., Verschuuren, M. A. & Polman, A. Broadband omnidirectional antireflection coating based on subwavelength surface Mie resonators. *Nat Commun* **3**, doi:Artn 692 Doi 10.1038/Ncomms1691 (2012).

23 Liu, S. *et al.* Optical magnetic mirrors without metals. *Optica* **1**, 250-256, doi:10.1364/Optica.1.000250 (2014).

24 Lewi, T., Iyer, P. P., Butakov, N. A., Mikhailovsky, A. A. & Schuller, J. A. Widely Tunable Infrared Antennas Using Free Carrier Refraction. *Nano letters* **15**, 8188-8193, doi:10.1021/acs.nanolett.5b03679 (2015).

25 Iyer, P. P., Pendharkar, M. & Schuller, J. A. Electrically Reconfigurable Metasurfaces Using Heterojunction Resonators. *Adv Opt Mater* **4**, 1582-1588, doi:10.1002/adom.201600297 (2016).

26 Fischer, M. P. *et al.* Optical Activation of Germanium Plasmonic Antennas in the Mid-Infrared. *Physical review letters* **117**, 047401, doi:10.1103/PhysRevLett.117.047401 (2016).

27 Shcherbakov, M. R. *et al.* Ultrafast all-optical tuning of direct-gap semiconductor metasurfaces. *Nat Commun* **8**, 17, doi:10.1038/s41467-017-00019-3 (2017).

28 Parry, M. *et al.* Active tuning of high-Q dielectric metasurfaces. *Appl Phys Lett* **111**, doi:Artn 053102 10.1063/1.4997301 (2017).

29 Li, S.-Q. *et al.* Phase-only transmissive spatial light modulator based on tunable dielectric metasurface. *Science* **364**, 1087, doi:10.1126/science.aaw6747 (2019).

30 Bar-David, J., Stern, L. & Levy, U. Dynamic Control over the Optical Transmission of Nanoscale Dielectric Metasurface by Alkali Vapors. *Nano letters* **17**, 1127-1131, doi:10.1021/acs.nanolett.6b04740 (2017).

31 Forouzmand, A., Salary, M. M., Inampudi, S. & Mosallaei, H. A Tunable Multigate Indium-Tin-Oxide-Assisted All-Dielectric Metasurface. *Adv Opt Mater* **6**, doi:Artn 1701275 10.1002/Adom.201701275 (2018).

32 Howes, A., Wang, W. Y., Kravchenko, I. & Valentine, J. Dynamic transmission control based on all-dielectric Huygens metasurfaces. *Optica* **5**, 787-792, doi:10.1364/Optica.5.000787 (2018).

33 Wang, Q. *et al.* Optically reconfigurable metasurfaces and photonic devices based on phase change materials. *Nat Photon* **10**, 60-65, doi:10.1038/nphoton.2015.247 2016).

34 Tian, J. *et al.* Active control of anapole states by structuring the phase-change alloy Ge2Sb2Te5. *Nature Communications* **10**, 396, doi:10.1038/s41467-018-08057-1 (2019).

35 Kamali, S. M., Arbabi, E., Arbabi, A., Horie, Y. & Faraon, A. Highly tunable elastic dielectric metasurface lenses. *Laser Photonics Rev* **10**, 1002-1008, doi:10.1002/lpor.201600144 (2016).

36 Arbabi, E. *et al.* MEMS-tunable dielectric metasurface lens. *Nat Commun* **9**, 812, doi:10.1038/s41467-018-03155-6 (2018).

37 She, A., Zhang, S., Shian, S., Clarke, D. R. & Capasso, F. Adaptive metalenses with simultaneous electrical control of focal length, astigmatism, and shift. *Science Advances* **4**, doi:10.1126/sciadv.aap9957 (2018).

38 Lewi, T., Evans, H. A., Butakov, N. A. & Schuller, J. A. Ultrawide Thermo-optic Tuning of PbTe Meta-Atoms. *Nano letters* **17**, 3940-3945, doi:10.1021/acs.nanolett.7b01529 (2017).

39 Iyer, P. P., Pendharkar, M., Palmstrøm, C. J. & Schuller, J. A. Ultrawide thermal free-carrier tuning of dielectric antennas coupled to epsilon-near-zero substrates. *Nat Commun* **8**, 472, doi:10.1038/s41467-017-00615-3 (2017).

40 Iyer, P. P., DeCrescent, R. A., Lewi, T., Antonellis, N. & Schuller, J. A. Uniform Thermo-Optic Tunability of Dielectric Metalenses. *Physical Review Applied* **10**, 044029, doi:10.1103/PhysRevApplied.10.044029 (2018).
41 Lewi, T. *et al.* Thermally Reconfigurable Meta-Optics. *IEEE Photonics Journal* **11**, 1-16, doi:10.1109/JPHOT.2019.2916161 (2019).
42 Rahmani, M. *et al.* Reversible Thermal Tuning of All-Dielectric Metasurfaces. *Adv Funct Mater* **27**, n/a-n/a, doi:10.1002/adfm.201700580 (2017).
43 Iyer, P. P., DeCrescent, R. A., Lewi, T., Antonellis, N. & Schuller, J. A. Uniform Thermo-Optic Tunability of Dielectric Metalenses. *Physical Review Applied* **10**, doi:10.1103/PhysRevApplied.10.044029 (2018).
44 Butakov, N. A. *et al.* Broadband Electrically Tunable Dielectric Resonators Using Metal-Insulator Transitions. *Acs Photonics*, doi:10.1021/acsphotonics.8b00699 (2018).
45 Ruggeri, F. S. *et al.* Infrared nanospectroscopy characterization of oligomeric and fibrillar aggregates during amyloid formation. *Nature Communications* **6**, 7831, doi:10.1038/ncomms8831 (2015).
46 Tittl, A. *et al.* A Switchable Mid-Infrared Plasmonic Perfect Absorber with Multispectral Thermal Imaging Capability. *Advanced Materials* **27**, 4597-4603, doi:10.1002/adma.201502023 (2015).
47 Adato, R. & Altug, H. In-situ ultra-sensitive infrared absorption spectroscopy of biomolecule interactions in real time with plasmonic nanoantennas. *Nature Communications* **4**, 2154, doi:10.1038/ncomms3154 (2013).
48 Ostendorf, R. *et al.* Recent Advances and Applications of External Cavity-QCLs towards Hyperspectral Imaging for Standoff Detection and Real-Time Spectroscopic Sensing of Chemicals. *Photonics* **3**, doi:10.3390/photonics3020028 (2016).
49 Lewi, T. & Katzir, A. Silver halide single-mode strip waveguides for the mid-infrared. *Optics Letters* **37**, 2733-2735, doi:10.1364/OL.37.002733 (2012).
50 Zilberman, S., Ravid, A., Katzir, A. & Lewi, T. Fiber-Optic Evanescent Wave Spectroscopy of Subsurface Layers of Solid Propellant Combustion. *Journal of Propulsion and Power* **32**, 1119-1123, doi:10.2514/1.B35956 (2016).
51 Lobel, B., Eyal, O., Kariv, N. & Katzir, A. Temperature controlled CO2 laser welding of soft tissues: Urinary bladder welding in different animal models (rats, rabbits, and cats). *Lasers in Surgery and Medicine* **26**, 4-12, doi:10.1002/(SICI)1096-9101(2000)26:1<4::AID-LSM3>3.0.CO;2-J (2000).
52 Yao, Y., Hoffman, A. J. & Gmachl, C. F. Mid-infrared quantum cascade lasers. *Nature Photonics* **6**, 432, doi:10.1038/nphoton.2012.143 (2012).
53 Lewi, T., Shalem, S., Tsun, A. & Katzir, A. Silver halide single-mode fibers with improved properties in the middle infrared. *Applied Physics Letters* **91**, 251112, doi:10.1063/1.2827195 (2007).
54 Lewi, T., Tsun, A., Katzir, A., Kaster, J. & Fuchs, F. Silver halide single mode fibers for broadband middle infrared stellar interferometry. *Applied Physics Letters* **94**, 261105, doi:10.1063/1.3166864 (2009).
55 Lewi, T., Ofek, J. & Katzir, A. Antiresonant reflecting microstructured optical fibers for the mid-infrared. *Applied Physics Letters* **102**, 101104, doi:10.1063/1.4795533 (2013).
56 Nguyen, H.-D. *et al.* Low-loss 3D-laser-written mid-infrared LiNbO3 depressed-index cladding waveguides for both TE and TM polarizations. *Optics Express* **25**, 3722-3736, doi:10.1364/OE.25.003722 (2017).
57 Dasgupta, S., Broderick, N. G. R., Richardson, D. J., Lewi, T. & Katzir, A. Improved method for estimating the minimum length of modal filters fabricated for stellar interferometry. *Optics Express* **17**, 1935-1946, doi:10.1364/OE.17.001935 (2009).
58 Grille, R. *et al.* Comparative study of mid-infrared fibers for modal filtering. *Applied Optics* **49**, 6340-6347, doi:10.1364/AO.49.006340 (2010).

59 Ksendzov, A. *et al.* Modal filtering for midinfrared nulling interferometry using single mode silver halide fibers. *Applied Optics* **47**, 5728-5735, doi:10.1364/AO.47.005728 (2008).

60 Grille, R. *et al.* Single mode mid-infrared silver halide asymmetric flat waveguide obtained from crystal extrusion. *Optics Express* **17**, 12516-12522, doi:10.1364/OE.17.012516 (2009).

61 Ghosh, G. *Handbook of optical constants of solids: Handbook of thermo-optic coefficients of optical materials with applications*. (Academic Press, 1998).

62 Lewi, T., Butakov Nikita, A. & Schuller Jon, A. in *Nanophotonics* Vol. 8 331 (2019).

63 Butakov, N. A. *et al.* Switchable Plasmonic–Dielectric Resonators with Metal–Insulator Transitions. *Acs Photonics* **5**, 371-377, doi:10.1021/acsphotonics.7b00334 (2017).

64 Lewi, T., Evans, H. A., Butakov, N. A. & Schuller, J. A. Ultrawide Thermo-optic Tuning of PbTe Meta-Atoms. *Nano Letters* **17**, 3940-3945, doi:10.1021/acs.nanolett.7b01529 (2017).

65 Zemel, J. N., Jensen, J. D. & Schoolar, R. B. Electrical and Optical Properties of Epitaxial Films of Pbs Pbse Pbte and Snte. *Phys Rev* **140**, A330-&, doi:DOI 10.1103/PhysRev.140.A330 (1965).

66 Gibbs, Z. M. *et al.* Temperature dependent band gap in PbX (X = S, Se, Te). *Appl Phys Lett* **103**, doi:Artn 262109 10.1063/1.4858195 (2013).

67 Sautter, J. *et al.* Active Tuning of All-Dielectric Metasurfaces. *ACS nano*, doi:10.1021/acsnano.5b00723 (2015).

68 Makarov, S. *et al.* Tuning of Magnetic Optical Response in a Dielectric Nanoparticle by Ultrafast Photoexcitation of Dense Electron-Hole Plasma. *Nano letters* **15**, 6187-6192, doi:10.1021/acs.nanolett.5b02534 (2015).

69 Shcherbakov, M. R. *et al.* Ultrafast All-Optical Switching with Magnetic Resonances in Nonlinear Dielectric Nanostructures. *Nano letters* **15**, 6985-6990, doi:10.1021/acs.nanolett.5b02989 (2015).

70 Baranov, D. G. *et al.* Nonlinear Transient Dynamics of Photoexcited Resonant Silicon Nanostructures. *Acs Photonics* **3**, 1546-1551, doi:10.1021/acsphotonics.6b00358 (2016).

71 Piccioli, N., Besson, J. M. & Balkanski, M. Optical-Constants and Band-Gap of Pbte from Thin-Film Studies between 25 and 300degrees K. *J Phys Chem Solids* **35**, 971-977, doi:Doi 10.1016/S0022-3697(74)80107-1 (1974).

72 Weiting, F. & Yixun, Y. Temperature Effects on the Refractive-Index of Lead-Telluride and Zinc Selenide. *Infrared Phys* **30**, 371-373, doi:Doi 10.1016/0020-0891(90)90055-Z (1990).

73 Tauber, R. N., Machonis, A. A. & Cadoff, I. B. Thermal and Optical Energy Gaps in PbTe. *J Appl Phys* **37**, 4855-4860, doi:doi:http://dx.doi.org/10.1063/1.1708150 (1966).

74 Wuttig, M., Bhaskaran, H. & Taubner, T. Phase-change materials for non-volatile photonic applications. *Nature Photonics* **11**, 465, doi:10.1038/nphoton.2017.126 (2017).

75 Li, P. *et al.* Reversible optical switching of highly confined phonon–polaritons with an ultrathin phase-change material. *Nature Materials* **15**, 870, doi:10.1038/nmat4649 (2016).

76 Goldflam, M. D. *et al.* Voltage switching of a VO2 memory metasurface using ionic gel. *Applied Physics Letters* **105**, 041117, doi:10.1063/1.4891765 (2014).

77 Rensberg, J. *et al.* Active Optical Metasurfaces Based on Defect-Engineered Phase-Transition Materials. *Nano Letters* **16**, 1050-1055, doi:10.1021/acs.nanolett.5b04122 (2016).

78 Liu, M. *et al.* Terahertz-field-induced insulator-to-metal transition in vanadium dioxide metamaterial. *Nature* **487**, 345, doi:10.1038/nature11231 (2012).

79 Zhu, Z., Evans, P. G., Haglund, R. F. & Valentine, J. G. Dynamically Reconfigurable Metadevice Employing Nanostructured Phase-Change Materials. *Nano Letters* **17**, 4881-4885, doi:10.1021/acs.nanolett.7b01767 (2017).

80 Liu, L., Kang, L., Mayer, T. S. & Werner, D. H. Hybrid metamaterials for electrically triggered multifunctional control. *Nature Communications* **7**, 13236, doi:10.1038/ncomms13236 (2016).

81 Kalcheim, Y. *et al.* Robust Coupling between Structural and Electronic Transitions in a Mott Material. *Physical Review Letters* **122**, 057601, doi:10.1103/PhysRevLett.122.057601 (2019).
82 McLeod, A. S. *et al.* Nanotextured phase coexistence in the correlated insulator V2O3. *Nature Physics* **13**, 80, doi:10.1038/nphys3882 (2016).
83 Lewi, T. *et al.* Thermally reconfigurable meta-optics. *IEEE Photonics Journal*, 1-1, doi:10.1109/JPHOT.2019.2916161 (2019).